

ORIGINAL ARTICLE



Reduction in Pulmonary Vein Stenosis and Collateral Damage With Pulsed Field Ablation Compared With Radiofrequency Ablation in a Canine Model

Brian Howard, PhD; David E. Haines, MD; Atul Verma¹, MD; Douglas Packer², MD; Nicole Kirchhof³, DVM, ACVP; Noah Barka⁴, DVM; Birce Onal⁵, PhD; Steve Fraasch, MS; Damijan Miklavčič⁶, PhD; Mark T. Stewart⁷, BS

BACKGROUND: Pulmonary vein (PV) stenosis is a highly morbid condition that can result after catheter ablation for PV isolation. We hypothesized that pulsed field ablation (PFA) would reduce PV stenosis risk and collateral injury compared with irrigated radiofrequency ablation (IRF).

METHODS: IRF and PFA deliveries were randomized in 8 dogs with 2 superior PVs ablated using one technology and 2 inferior PVs ablated using the other technology. IRF energy (25–30 W) or PFA was delivered (16 pulse trains) at each PV in a proximal and in a distal site. Contrast computed tomography scans were collected at 0, 2, 4, 8, and 12-week (termination) time points to monitor PV cross-sectional area at each PV ablation site.

RESULTS: Maximum average change in normalized cross-sectional area at 4-weeks was $-46.1 \pm 45.1\%$ post-IRF compared with $-5.5 \pm 20.5\%$ for PFA ($P \leq 0.001$). PFA-treated targets showed significantly fewer vessel restrictions compared with IRF ($P \leq 0.023$). Necropsy showed expansive PFA lesions without stenosis in the proximal PV sites, compared with more confined and often incomplete lesions after IRF. At the distal PV sites, only IRF ablations were grossly identified based on focal fibrosis. Mild chronic parenchymal hemorrhage was noted in 3 left superior PV lobes after IRF. Damage to vagus nerves as well as evidence of esophagus dilation occurred at sites associated with IRF. In contrast, no lung, vagal nerve, or esophageal injury was observed at PFA sites.

CONCLUSIONS: PFA significantly reduced risk of PV stenosis compared with IRF postprocedure in a canine model. IRF also caused vagus nerve, esophageal, and lung injury while PFA did not.

GRAPHIC ABSTRACT: A graphic abstract is available for this article.

Key Words: atrial fibrillation ■ cardiac electrophysiology ■ catheter ablation ■ dilation ■ pulmonary vein stenosis

Atrial fibrillation (AF) is a heterogeneous disease associated with high morbidity and mortality that will affect >12 million in the United States by 2050.^{1–3} Catheter ablation to isolate the pulmonary veins (PVs) is an effective therapy for patients with symptomatic AF typically using radiofrequency energy. If radiofrequency

is delivered within the PVs, there is a risk of causing thermal damage to the walls of the PV ostium, leading to stenosis⁴ which can present as pulmonary hypertension, lung infarction, or hemoptysis.^{5–8} Other complications from radiofrequency deliveries include steam pops, perforation, thrombus, and injury to collateral tissue such

Correspondence to: Mark T. Stewart, BS, Medtronic—MVS46, 8200 Coral Sea St NE, Mounds View, MN 55112. Email mark.stewart@medtronic.com
For Sources of Funding and Disclosures, see page 919.

© 2020 The Authors. *Circulation: Arrhythmia and Electrophysiology* is published on behalf of the American Heart Association, Inc., by Wolters Kluwer Health, Inc. This is an open access article under the terms of the [Creative Commons Attribution Non-Commercial-NoDerivs](#) License, which permits use, distribution, and reproduction in any medium, provided that the original work is properly cited, the use is noncommercial, and no modifications or adaptations are made.

Circulation: Arrhythmia and Electrophysiology is available at www.ahajournals.org/journal/circep

WHAT IS KNOWN?

- Irrigated radiofrequency deliveries to isolate the pulmonary veins (PVs) can produce thermal injuries leading to PV stenosis and collateral injury to the lungs leading to hemoptysis or lung infarction.
- Pulsed field ablation creates lesions through the nonthermal mechanism of irreversible electroporation which has been shown to reduce or eliminate collateral injuries that are observed from radiofrequency ablations.

WHAT THE STUDY ADDS?

- A more precise method of evaluating PV stenosis was developed that includes the use of 3-dimensional modeling based on computed tomography angiography with triplicate measures of cross-sectional area at the distal PV and ostial ablation sites.
- PV measurements were made preablation and at 2, 4, 8, and 12 weeks postablation to provide a detailed time course of the progression of PV stenosis from radiofrequency ablations while showing negligible changes in dimensions in pulsed field ablation treated sites.
- We present on collateral injury to the lungs, esophagus, and vagus nerves from radiofrequency deliveries within the PVs which were not present where pulsed field ablation was delivered.

Nonstandard Abbreviations and Acronyms

| | |
|------------|--------------------------|
| AF | atrial fibrillation |
| CT | computed tomography |
| IRF | irrigated radiofrequency |
| PFA | pulsed field ablation |
| PV | pulmonary vein |
| PVS | pulmonary vein stenosis |

as the esophagus, coronary arteries, and phrenic nerves.⁹ Clinically, a threshold reduction of >70% of vessel diameter compared with the preablation baseline is considered severely stenosed with lesser grades characterized as moderately or mildly stenosed.^{5,9}

Preliminary results suggest that pulsed field ablation (PFA) may be a promising therapy for endocardial catheter ablation with the potential to reduce complications compared with standard AF ablation technologies.^{10–14} PFA applies pulsed electric fields to increase cell membrane permeability and invoke cell death through the mechanism of irreversible electroporation.^{15,16} Previous preclinical studies have found minimal impact on PV diameters after irreversible electroporation energy deliveries based on single measurements of PV diameter.^{17–19} We aimed to more precisely quantify the effects of PFA versus an irrigated radiofrequency (IRF) control

on the time course of pulmonary vein stenosis (PVS) in a chronic canine preclinical model using a novel method with 3-dimensional modeling based on computed tomography (CT) angiography of the PVs at multiple time points postablation.

METHODS

Animals and Preablation Procedures

The data that support the findings of this study are available from the corresponding author upon reasonable request. This preclinical study was conducted at Medtronic's Physiological Research Laboratories (Minneapolis, MN), certified by the Association for Assessment and Accreditation of Laboratory Animal Care. The study protocol was approved by the Institutional Animal Care and Use Committee and conformed to the Guide for Care and Use of laboratory Animals. Eight fully grown mongrel hound subjects (27.9 ± 3.2 kg, 6 females and 2 males) underwent a baseline PV CT angiogram within 10 days before the procedure. The day before surgery through 3 days after surgery, animals were given carprofen (4 mg/kg PO), fentanyl (50 µg/h transdermal), and buprenorphine (0.01 mg/kg IM) for analgesia. Oral amiodarone was administered (5 mg/kg PO BID) for 3 days before surgery. On the day of surgery, morphine (1 mg/kg IM) and acepromazine (1 mg IM) were administered, and anesthesia was induced with propofol (2.5–4 mg/kg IV). Cefazolin (22.5 mg/kg IV) was given prophylactically. Each dog was maintained at an appropriate plane of anesthesia with isoflurane (0.5%–2.5%). Heparin (175–250 units/kg IV) was administered to maintain the activated clotting time at a minimum of 350 s.

A rotational angiogram (Artis Zee, Siemens Healthcare) of the pulmonary vasculature was collected before the ablation procedure to provide images of the individual PV anatomy and navigate to optimal targets for ablation and subsequent measurement. After venous femoral access and transseptal puncture, a steerable sheath (FlexCath Select Steerable Sheath, 10 Fr, Medtronic) was placed into the left atrium.

Catheter Ablation of the PVs

Superior and inferior PVs were selected in each of the 8 dogs to receive either IRF or PFA at both superior locations, and the other energy modality in both inferior locations. Larger vessels were used as the ablation targets to reduce measurement error. In each treated vein, the selected ablation modality was applied in both proximal or distal locations to allow assessment of PV stenosis as well as collateral damage to lungs and nerves beyond the vascular targets (Figure 1A and 1B). The energy application sites were intentionally designed as a worst-case scenario and not meant to replicate standard clinical practice. To ensure accurate and consistent positioning, all catheter placements were guided by rotational angiography and performed by an experienced operator. All 8 subjects received treatment within a 4-day period.

For PFA applications, a 9-electrode circular array PV ablation catheter (GOLD, Medtronic) was powered by a custom PFA research generator that was designed for future human clinical use (URL: <https://www.clinicaltrials.gov>; Unique identifier: NCT04198701). This generator delivered trains of short,

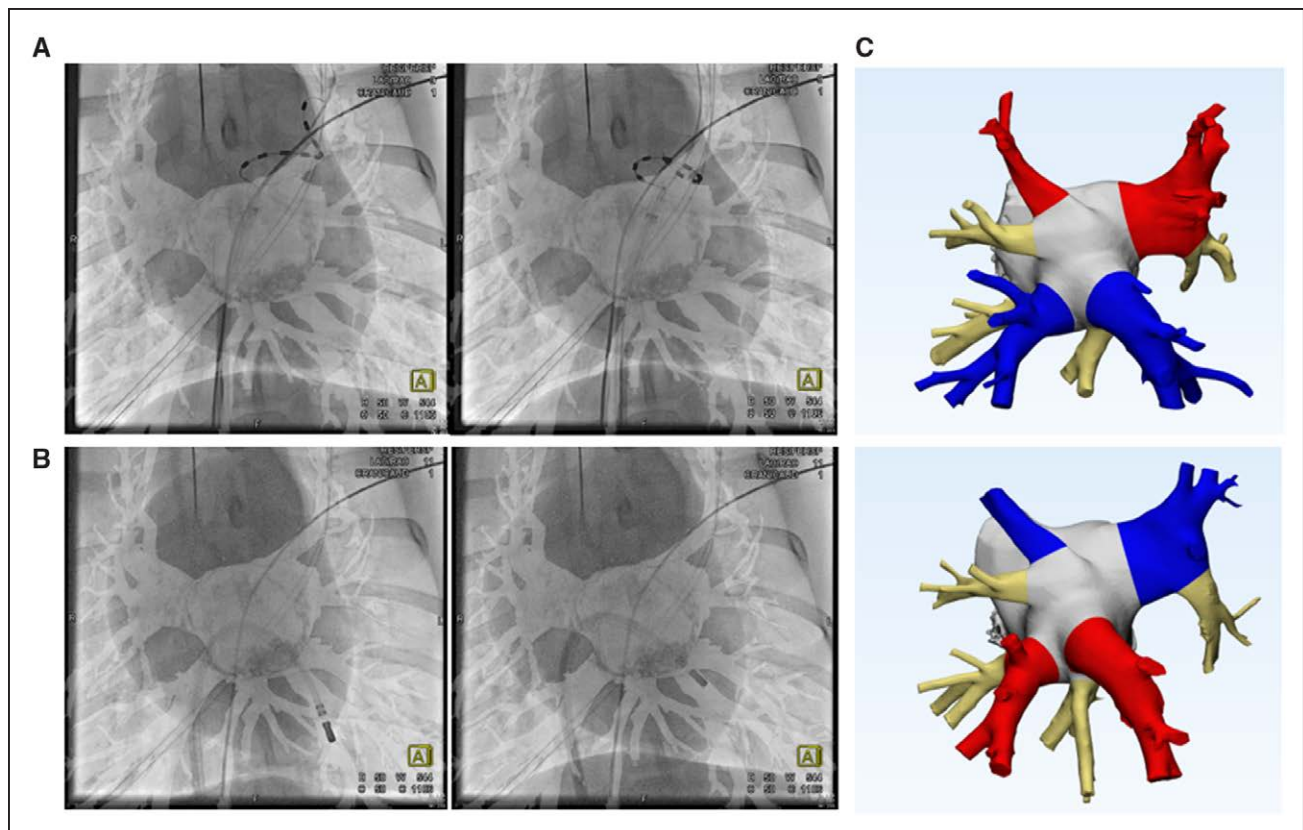


Figure 1. Rotational angiography was used for catheter positioning and serial computed tomography imaging for chronic pulmonary vein (PV) anatomical measurements.

Distal (**left**) and proximal (**right**) ablations were performed for the pulsed field ablation (**A**) and irrigated radiofrequency catheters (**B**). Examples of 3-dimensional models (**C**) were based on serial contrast imaging at baseline and each chronic time point with identified ablation sites for PV cross-sectional area measurements. Red (irrigated radiofrequency [IRF]), blue (pulsed field ablation [PFA]), and beige (control) indicate randomized treatments of IRF or PFA to be received by the superior or inferior PVs in these baseline examples.

high-voltage (1500 V), biphasic pulses to the multielectrode catheter.²⁰ At each proximal PV site and then at each distal PV site, the catheter was rotated and positioned 4× for each PFA application of 4 pulse trains. The intent was to expose the PV lumens and all of the surrounding tissue to repeated PFA deliveries, including significant overlap of these energy deliveries by spiraling the electrode array into each PV ostium as well as more distally into the narrow, constrained canine PVs. More precisely, this included at each PV ostium, 4 array placements (rotated between placements) with 4 pulse trains per placement, resulting in 16 pulse trains applied at each PV ostium. This was followed by spiraling the array more distally into each PV, rotating the array within each distal PV to 4 distinct placements with 4 pulse trains delivered per placement, resulting in 16 pulse trains being delivered within each distal PV, deep within the lungs. The system was connected to a cardiac R-wave monitor to gate pulse train deliveries during the ventricular refractory period.^{21,22}

IRF applications were performed using a THERMOCOOL (Biosense-Webster) catheter powered by with an Atakr II radiofrequency generator (Medtronic), irrigated with a CoolFlow (Biosense-Webster) pump. In distal PV locations, IRF was delivered at 25 to 30 watts (W) in a circumferential pattern for up to 2 minutes total duration (1.91 ± 0.21 minutes) with an irrigation flow of 25 to 30 mL/min. In proximal PV locations, the same power was applied for up to 4 minutes (3.88 ± 0.55 minutes) with an irrigation flow of 17 to 30 mL/min. No attempt was made to assess for electrical

isolation of the PV muscle sleeves. Once all ablations were completed, the canines were recovered under veterinary supervision and followed for 12 weeks (83–85 days). No postprocedure anticoagulation or antiplatelet therapy was administered during the 12-week survival period. Follow-up cardiac-gated contrast CT scans were performed at 2, 4, 8, and at the 12-week termination. To enhance visualization of lesions during gross necropsy, TTC (10 mL of 10% TTC by weight) was administered intravenously, 5 minutes before euthanasia. Each canine was euthanized by introducing an electrophysiology catheter into the right ventricle and applying 9 V DC to induce ventricular fibrillation.

Three-Dimensional Modeling and Measurement of PV Cross-Sectional Area

An independent technician blinded to the site treatments was responsible for generating the 3-dimensional model of each PV anatomy based on the cardiac CT scans using Mimics software (Materialise, Leuven, Belgium; Figure 1C). Measurements were made of PV cross-sectional areas to document venous narrowing or stenosis at each ablation site ($n=16$ proximal and $n=16$ distal sites). PV anatomy at each time point was measured in a blinded manner in triplicate by the same analyst. Cross-sectional measurements were made from the blood volume model's centerline. Cross-sectional area was used for statistical analysis as a more precise and robust measurement of PV reduction over time as opposed to multiple diameter measurements.

Control vessels were identified and measured at positions neighboring each of the main pulmonary vessels that received ablations. These vessels did not receive IRF or PFA and received no intended catheter manipulations within the anatomy. The control vessels provided a means of normalizing variations in the model due to differences in CT scan contrast brightness, modeling settings, animal growth, and weight loss/disease.

Pathology

Pathology analysis was performed by one board-certified, veterinary pathologist, experienced in device pathology, and blinded to the assignment of ablation modality for each sample.²³ At necropsy, the heart, treated lung lobes, and adjacent esophagus and vagus nerves were examined. After fixation in 10% neutral buffered formalin, tissues were trimmed and pertinent PV, lung, esophagus and vagal nerve sections, each previously marked in necropsy to maintain spatial context, were forwarded for histology. Specimens were dehydrated, paraffin embedded, and sectioned at $\approx 4 \mu\text{m}$. Slides were stained with hematoxylin and eosin and Masson trichrome. Histopathologic assessment included evaluation of local healing response including presence of endocardial thrombus. Moreover, collateral pathological findings interpreted as ablation sequelae were diagnosed. It was not the pathology objective to correlate the percent-stenosis that was calculated from in vivo imaging modalities to PV histomorphometry.

Statistical Analysis

Measured values were reported as mean and standard deviations. Comparisons between populations with continuous measurements were performed as a 2-sample *t* test (Minitab Inc. State College, PA). Comparisons between binary characteristics were performed using Fischer exact test. A $P < 0.05$ was considered statistically significant.

RESULTS

Procedure Outcomes

Ablations were successfully performed at a total of 32 PVs treated in 8 canines. Seven canines were terminated after an average of 84.3 days (83–85 days) while one canine died early at 55 days. Neither ventricular arrhythmias nor AF were initiated by either energy source. IRF deliveries resulted in steam pops at 7 proximal and 3 distal positions. No coagulum was observed on the circular multielectrode catheters after PFA, but thermal coagulum deposits were observed on the catheters used for IRF in 4 instances. Seven of the 8 animals survived to the intended 12-week time point without clinical symptoms. The remaining animal expired during preparation for the 8-week CT scan due to an anesthesia incident unrelated to ablations or intercurrent disease.

Pulmonary Vein Stenosis

Baseline values for cross-sectional areas compared between all target locations were not significantly different between sites assigned to undergo IRF or PFA ($P = 0.797$). After ablation, significant PV stenosis was observed at the IRF ablation sites whereas none was seen with PFA (Figure 2). Complete occlusion of the vessel was observed in association with IRF deliveries, but not with PFA deliveries (Figure 3). The maximum average change in normalized cross-sectional area at 4 weeks post-IRF ablation (compared with baseline) was $-46.1 \pm 45.1\%$ compared with $-5.5 \pm 20.5\%$ for PFA at 4 weeks ($P \leq 0.001$). At the 4-week time point, severe stenosis was measured in 6 of 32 (18.8%) IRF sites and 0 of 32 (0%) PFA delivery sites ($P \leq 0.003$). An example

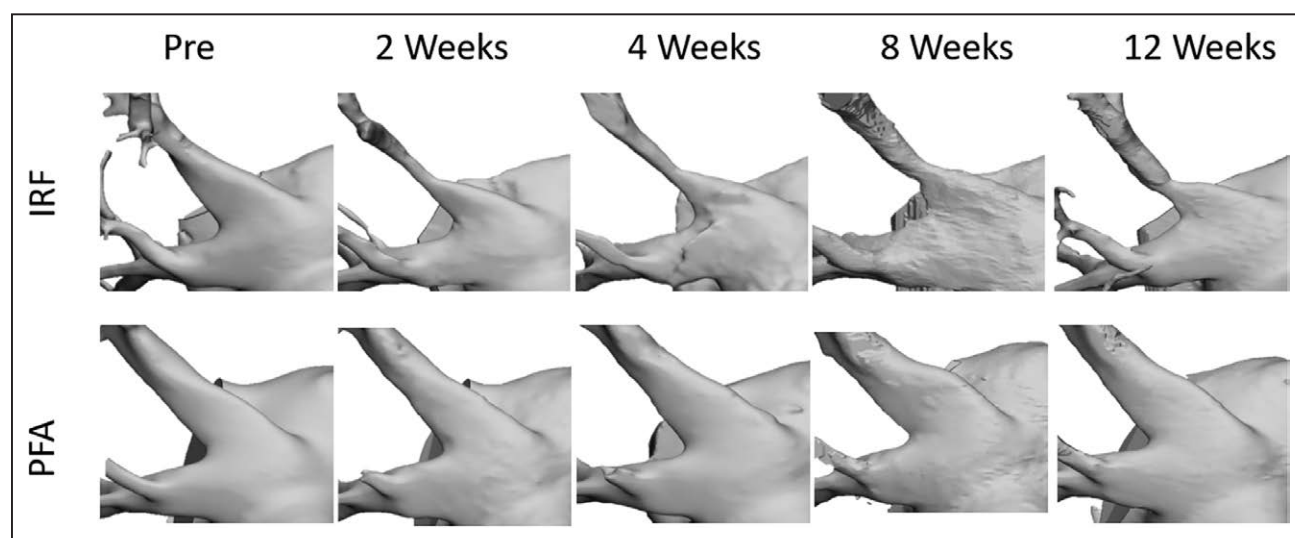


Figure 2. Three-dimensional model of 2 treated left superior pulmonary veins over 5 time points through the 12-week study. The **top** branch in each row was treated with either irrigated radiofrequency (IRF; **top** row) or pulsed field ablation (PFA; **bottom** row), and the **bottom** branch in each row served as a control vessel. Vessel constriction over time was assessed based on measurements of the cross-sectional area at the treated section, compared with preablation measurements (first column). Measurements were made immediately after the bifurcation in vessels. Control and PFA-treated vessels showed no change in diameter or $<10\%$ decrease in diameter over the 12 wk survival.

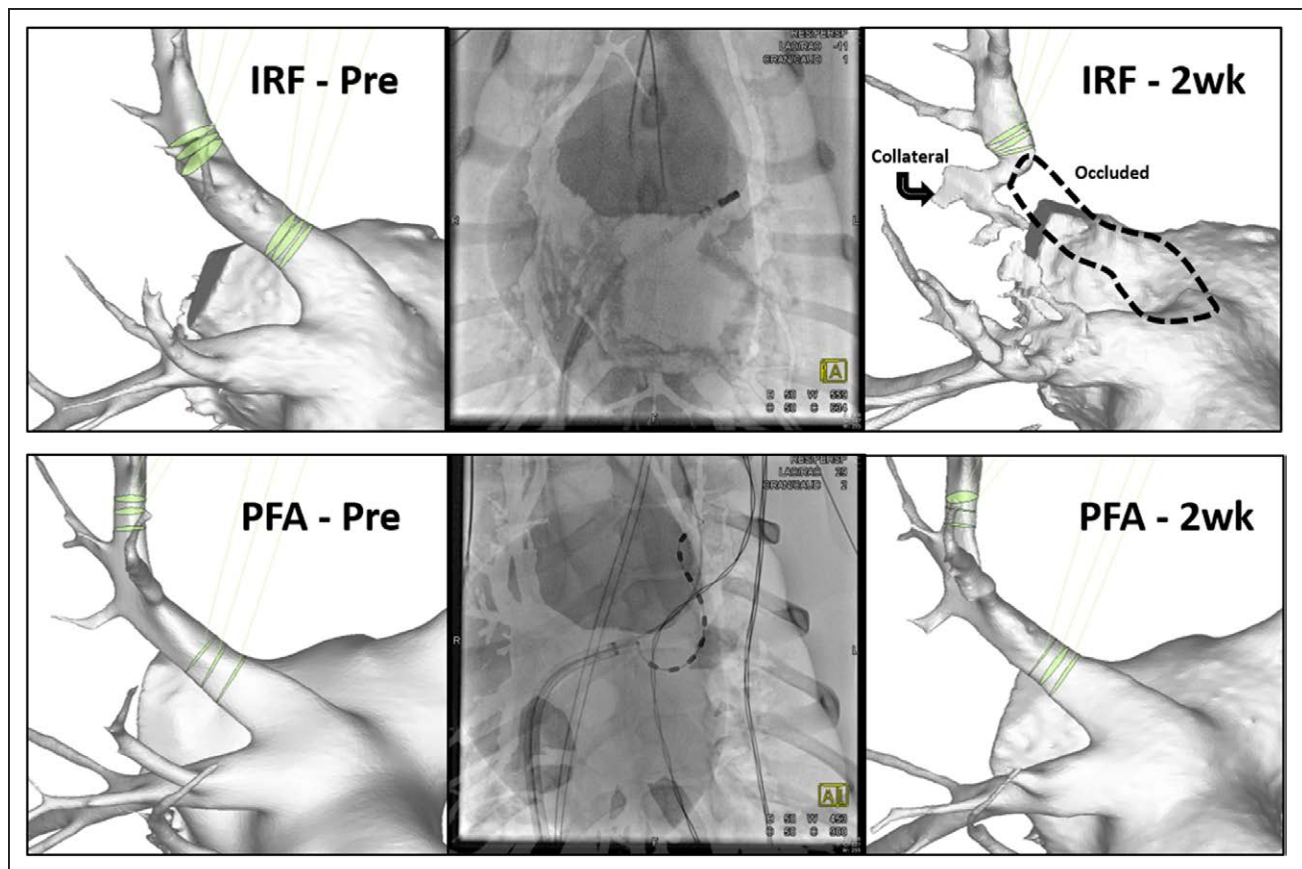


Figure 3. Three-dimensional model of 3 left superior pulmonary veins treated with irrigated radiofrequency (IRF; top row) or pulsed field ablation (PFA; bottom row) based on CT imaging.

At 2 weeks, IRF delivery resulted in complete occlusion of the vessel (**top right**). PFA delivery had no significant reduction of pulmonary vein cross-sectional area in the same anatomic target. Fluoroscopy image (**middle column**) demonstrates positioning of the PFA or IRF catheter. Proximal and distal ablation measurements are shown for each vein (green).

of the time course of PV cross-sectional area change over the 12-week duration is shown in Figure 4A and 4B.

A detailed analysis of proximal and distal sites for each energy form also demonstrates differences between the applied energies (Figure 4C). IRF and PFA treatment resulted in significant differences in cross-sectional area reduction at all time points in proximal sites ($P \leq 0.022$). PFA delivery in distal sites (1–4 cm into vein) demonstrated significantly less cross-sectional area reduction than IRF at each time point through 8 weeks ($P \leq 0.044$). Maximum area reduction occurred around the 2- to 4-week time points following IRF delivery at proximal (47.2% reduction) and distal (45% reduction) sites. Distal sites recovered at 8-week (20% reduction) time point and maintained this recovery at the 12-week analysis (18.9% reduction; Figure 4A).

Figure 4C summarizes the measured PV size changes (both diameter and cross-sectional area) over 12 weeks post-IRF and PFA as well as the untreated control vessels. Notably, there are 6 targets (19%) counted in the present study treated with IRF which experienced >70% diameter ($\approx 91\%$ cross-sectional area) reduction that may be defined as severely stenosed at 4 weeks postablation. PFA by contrast had no vessels (0%)

which showed more than a 20% reduction in vessel diameter which was similar to the untreated control vessels. Although some control vessels underwent minor changes in diameter and cross-sectional area, this may be due to the effect of nearby radiofrequency treatment or animal subject variation.

PV Ablations

There were 2 ablation sites created in each of the PVs: one in the ostium (proximal) and one farther distal in the vein, deeper into the lung (distal). Ablated proximal myocardial tissue areas after PFA were all (16/16) continuously circumferential and transmurally replaced by fibrosis, were larger than after IRF (Figure 5) and were devoid of gross stenosis and thrombus. In contrast, 7/16 IRF ablations were circumferentially incomplete. Distal ablations well beyond the PV myocardial sleeve were found upon gross inspection at 15/16 IRF sites but only at 1/16 PFA sites (Figure 6). This indicates that gross inspection of non-myocardial tissue treated with PFA resulted in minimal grossly visible effects of the ablation. Via histopathology, 15/16 IRF sites and 10/16 PFA sites were observed

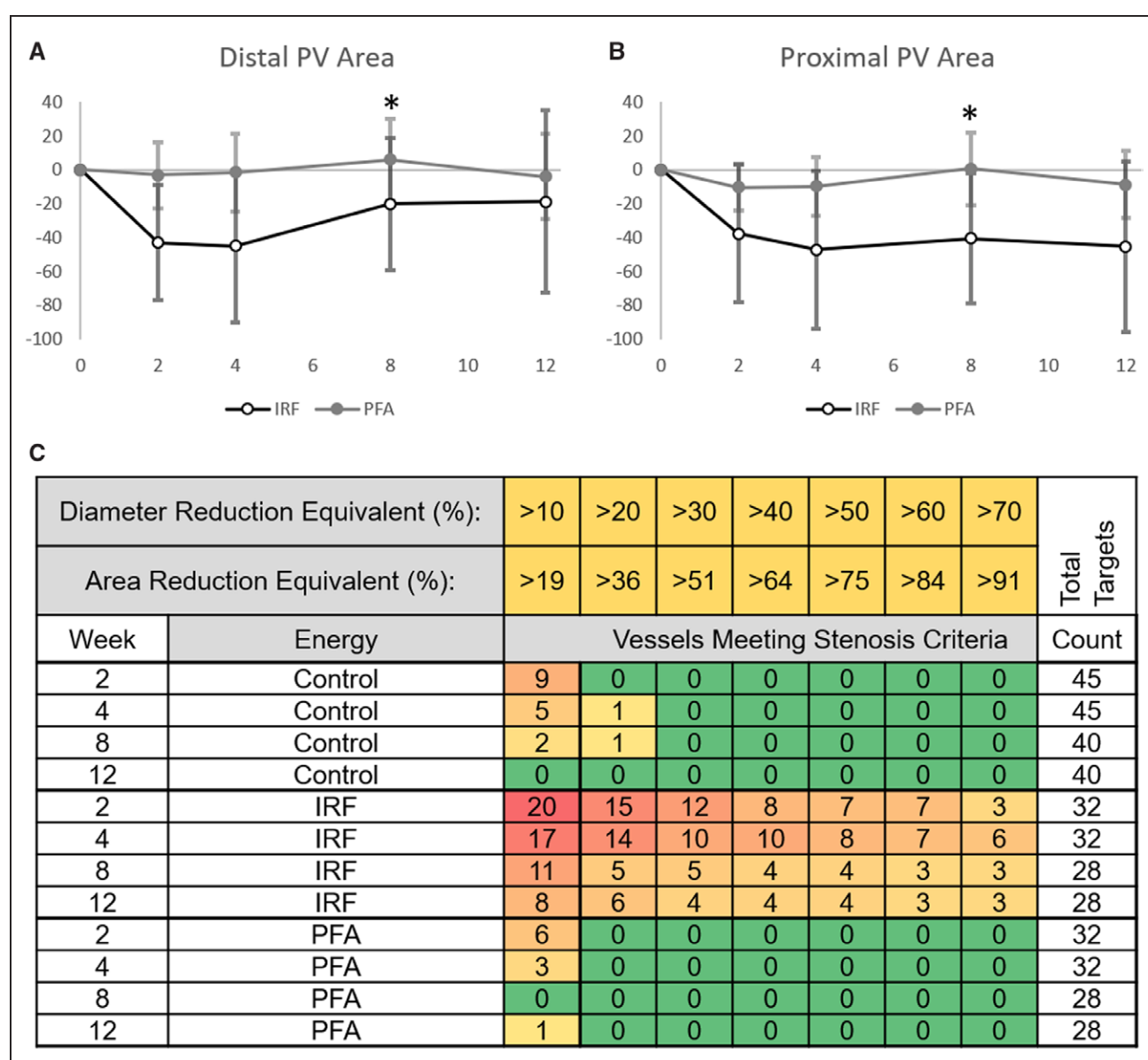


Figure 4. Pulmonary vein (PV) area and diameter changes for control vessels, irrigated radiofrequency (IRF)-treated PVs, and pulsed field ablation (PFA)-treated PVs followed from baseline to 12 weeks.

Time point 0 represents baseline before the ablation in the summary graphs of distal (A) and proximal (B) PV ablation sites showing that IRF reached the most severe diameter reduction at the 4-week time point and recovered (distal) or maintained the reduction (proximal) for the remainder of the study. The same degree of reduction was not observed in the PVs treated using PFA. One subject was lost at the 8-week time point (*). The numbers of graded control or ablation site assessments of PV stenosis are shown in C for control, IRF-treated, and PFA-treated vessels at each study time point. Vessels meeting a 10%–70% diameter reduction (equal to 19%–91% area reduction) were counted among the total number of targets measured (far right). Decreased number of total targets at the 8-week time point is due to one deceased animal. PFA-treated targets never exceeded a 10% diameter reduction from baseline after the 2-week time point while IRF-treated targets experienced all stenosis levels, from >10% to >70% reduction at all time points.

in distal nonmyocardial tissue locations. Detection of evidence of distal site PFA deliveries deep in the PVs consisted mainly of microscopic evidence of mild alveolar fibrosis surrounding the distal PV energy delivery sites. All of the detected myocardial ablation sites resulted in consistent replacement fibrosis of the muscular portion of the targeted PVs devoid of thrombus and with no noteworthy histopathologic differences between the 2 energy modalities at 12 weeks. Importantly, there were

no features that indicated adverse remodeling after PFA (eg, calcification, osseous metaplasia, vascular distortion, bronchiectasis, or emphysema). Large arteries in the vicinity of PFA lesions were normal.

Lung Tissue Damage

At necropsy, mild lung changes in the form of pleural fibrosis and hemosiderin discoloration was noted in three left

Table. PV Stenosis Measurements at IRF and PFA Ablation Sites Across all 12 Week of Chronic Survival

| | | Week | IRF | PFA | P Value |
|--|---------------------------|------|------------|-------------|---------|
| Starting vessel size | All, mm ² | 0 | 74.1±64 | 70.24±54.01 | 0.797 |
| | Distal, mm ² | 0 | 38.3±30.4 | 45.1±28.4 | 0.518 |
| | Proximal, mm ² | 0 | 109.8±69.4 | 95.4±62.3 | 0.540 |
| PV stenosis, % change vs baseline | Standard, % | 2 | −37.3±39.1 | −3.6±21.5 | <0.001 |
| | | 4 | −31.4±45.3 | 9.1±21.6 | <0.001 |
| | | 8 | −13.3±43.3 | 20.4±28.4 | 0.001 |
| | | 12 | −5.2±48.7 | 20.6±22.9 | 0.015 |
| | Normalized, % | 2 | −40.3±37 | −6.6±17 | <0.001 |
| | | 4 | −46.1±45.1 | −5.5±20.5 | <0.001 |
| | | 8 | −30.4±39.3 | 3.3±22.6 | <0.001 |
| | | 12 | −32.1±53 | −6.3±22.4 | 0.023 |
| | >70% reduction, n | 2 | 3/32 | 0/32 | 0.238 |
| | | 4 | 6/32 | 0/32 | 0.025 |
| | | 8 | 3/28 | 0/28 | 0.236 |
| | | 12 | 3/28 | 0/28 | 0.236 |
| PV stenosis distal, % change vs baseline | Normalized, % | 2 | −43±34.1 | −3.1±19.5 | <0.001 |
| | | 4 | −45±45.2 | −1.4±23 | 0.002 |
| | | 8 | −20.2±39 | 6±24.2 | 0.044 |
| | | 12 | −18.9±53.9 | −3.9±25 | 0.358 |
| PV stenosis proximal, % change vs baseline | Normalized, % | 2 | −37.6±40.6 | −10.2±13.7 | 0.020 |
| | | 4 | −47.2±46.5 | −9.7±17.3 | 0.007 |
| | | 8 | −40.6±38.4 | 0.7±21.5 | 0.002 |
| | | 12 | −45.3±50.4 | −8.7±20 | 0.022 |

Percent changes in vessel area are computed (standard), normalized to the control vessel measurements, and graded against current criteria for PVS, and assessed separately based on anatomic targets. Across all sites, PFA statistically significantly reduced PVS as compared with IRF regardless of the metric used. IRF indicates irrigated radiofrequency; PFA, pulsed field ablation; PV, pulmonary vein; and PVS, pulmonary vein stenosis.

superior pulmonary vein lobes after IRF treatment. Similar but lighter discoloration was observed in 3 of the PFA-treated right superior PV lobes. Fixed-tissue examination via cross sectioning of the lung at the distal ablation

sites (Figure 6) allowed for the identification of IRF but not PFA lesions as focal fibrosis. On histology, prominent alveolar fibrosis and damage to bronchi was only found after IRF treatment in nearby PVs. In 8 of them, there

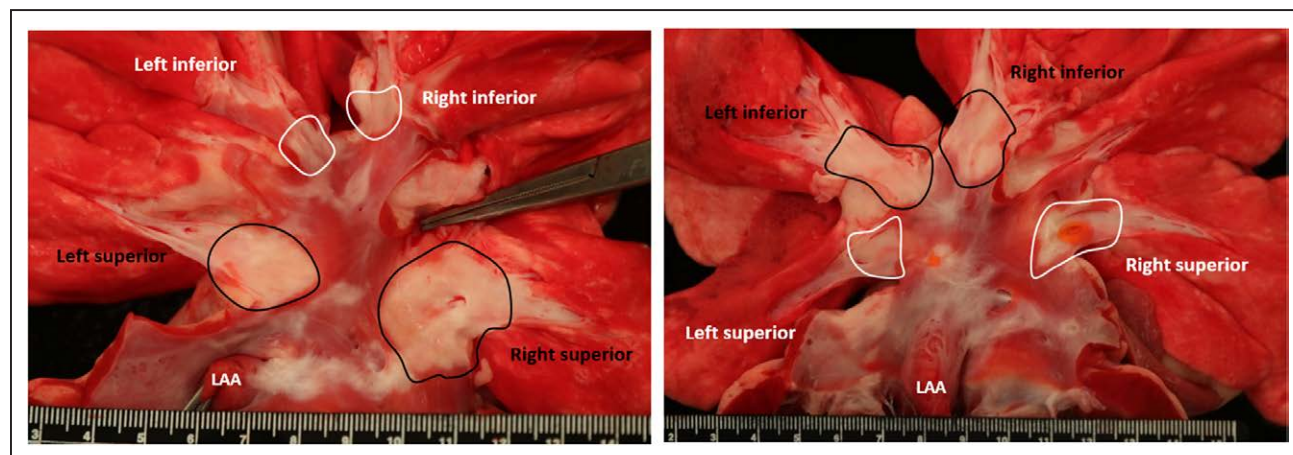


Figure 5. Necropsy findings, enhanced by TTC staining, of targeted pulmonary vein (PV) orifices (proximal) after pulsed field ablation (PFA; circled in black) or irrigated radiofrequency (IRF; circled in white) ablations 12 wk after treatment for 2 different subjects.

In the image on the **left**, the subject's inferior PVs were treated with PFA (white, circled) and superior PVs were treated with IRF (black, circled). In the image on the **right**, the subject's inferior PVs were treated with IRF (black, circled) and superior PVs were treated with PFA (white, circled). Rulers are in cm and mm units.

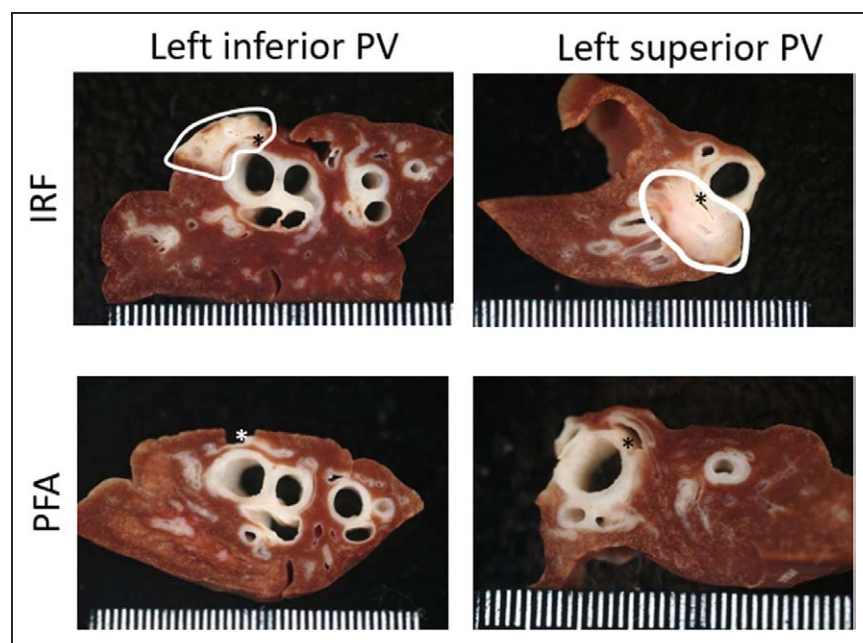


Figure 6. Fixed-tissue gross image panel with examples of cross sections through pulmonary lobes after irrigated radiofrequency (IRF) or pulsed field ablation (PFA) deliveries that were made distant (distal) to the venous orifices 12 wk earlier.

Clear evidence of collateral damage (circled) was observed in the IRF treated lobe, but no evidence of damage was found after PFA. Asterisks are inserted in or near pulmonary vein targets. PV indicates pulmonary vein.

was lingering necrosis with peripheral regeneration of the bronchial cartilage plates (Figure 7). In some IRF samples, the bronchial lumen was filled with mucus, the local smooth muscle was absent, or the bronchial epithelium had lost its native undulating pattern and was flat. Histology samples examined from grossly normal areas but corresponding to PFA treatment to PVs showed nearby lung tissue unaffected, apart from mild fibrosis.

Vagus Nerve Damage

Damage to the right and left vagus nerves was grossly observed in association with abutting IRF target sites at the inferior PVs only (Figure 8). Lesions were readily recognized as focal perineural fibrosis. All but one vagal nerve near these IRF targets were damaged, showing degeneration with severe endo- and peri-neural fibrosis on histology. These changes were not observed in any of the PFA counterparts. None of the vagal histology samples near PFA treatments demonstrated histopathologic changes such as Wallerian degeneration, inflammation, or axonal changes.

Esophageal Findings

Mild but noteworthy dilation of the esophagus was found in 3 animals that underwent bilateral IRF deliveries to their inferior PVs. This finding was attributed to the bilateral vagal nerve damage that occurred but caused no clinical symptoms.

DISCUSSION

The study demonstrated that PFA deliveries within the PVs did not result in significant PVS at any time point

during the 12 weeks follow-up. In contrast, IRF at similar sites resulted in significant PVS and sometimes complete PV occlusion. The PV narrowing effect of IRF peaked in the 2- to 4-week postablation time points with some veins showing mild recovery at 8- and 12-week time points. Animals were used as their own controls, and PFA-treated PV segments underwent minimal reduction in diameter and area (eg, none >20%, 36%, respectively) compared with the nonablated control segments during follow-up (Figure 4C). In addition, this study showed that in comparison to IRF, PFA showed no vagus nerve injury nor esophageal changes, and less damage to the lung parenchyma. This study was intentionally designed to target worst-case scenario application sites that do not replicate standard clinical practice, to test the safety profile of PFA in comparison to IRF.

Previous Studies

The prevalence of PV stenosis varies among reports, but a study of AF ablation reported 0.5% (52/10368 patients) significant (>70% diameter reduction) PV stenosis among patients undergoing contrast-enhanced spiral CT scans routinely at 3 to 6 months postablation to assess for PVS.^{24,25} The risk of PV stenosis decreases if ablation within the vein ostium is minimized, but ablations within the ostium may be unavoidable in some cases to completely isolate the veins. Since PV stenosis can be asymptomatic, the prevalence of PV stenosis may be significantly underestimated if routine imaging is not performed.⁵ A prior preclinical study reported a low incidence of PV stenosis with PV ablation performed with irreversible electroporation.^{17–19} Recent pilot trials have supported the safety of PFA with clinical ablation of PVs.^{12,13} The present study is the first quantitative direct comparison

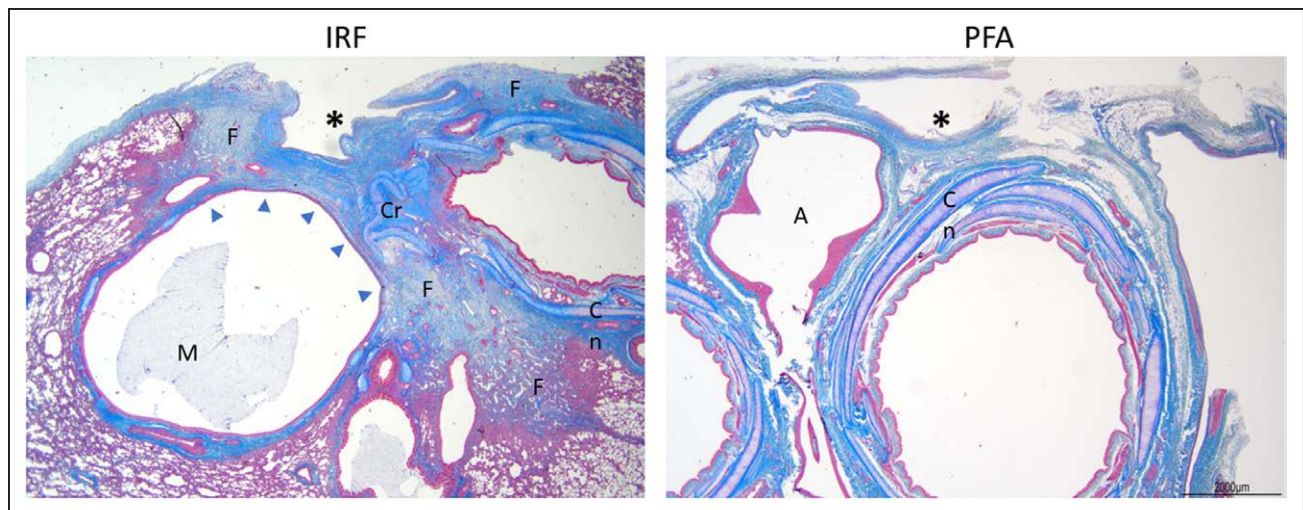


Figure 7. Photomicrographs of distal pulmonary veins (an asterisk marks each lumen) that were ablated with irrigated radiofrequency (IRF) or with pulsed field ablation (PFA) to evaluate potential chronic (12-week old) collateral damage. IRF ablations caused widespread perivenous fibrosis (F) with loss (arrow heads) and distortion of bronchiolar cartilage (C), as well as mucus (M) accumulation and epithelial flattening in nearby airways. No evidence of increased fibrosis or airway changes were noted after PFA. Masson trichrome stains. A indicates artery.

of PFA to IRF based on 3-dimensional measurements regarding the magnitude of PVS caused by ablation.

Mechanism of PV Stenosis

The mechanism of radiofrequency ablation tissue injury is thermal whereas the primary mechanism of cell death with PFA is irreversible electroporation, a disruption of the cell membrane permeability. The likely dominant

mechanism for PV stenosis after radiofrequency ablation is thermally mediated. Heating pulmonary venous tissues above 60°C causes contraction and loss of compliance coincident with collagen denaturation and disruption of its typical matrix.⁴ The effects were most certainly attributable to radiofrequency energy delivery rather than mechanical trauma due to catheter manipulation since no stenosis occurred with PFA, despite the introduction of a spiral electrode array deep into the PVs.

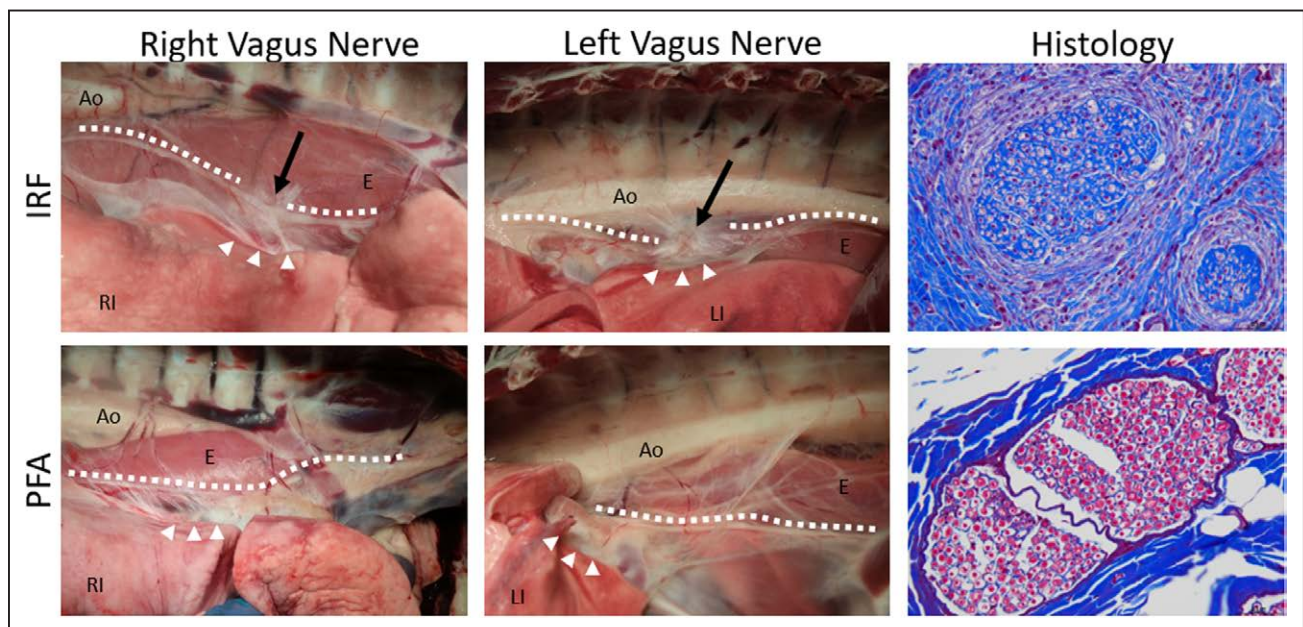


Figure 8. findings of the right and left vagus nerves (marked by dotted lines) after pulmonary vein ablations via irrigated radiofrequency (IRF; top row) or pulsed field ablation (PFA; bottom row) in the distal site of the ipsilateral pulmonary vein (arrow heads) 12 wk after treatment.

Juxtaposed to the IRF ablation sites, focally extensive fibrosis on the esophagus (E) that also involved the main vagus nerve branch (arrows) was noted in IRF 7/8 treatments. Affected vagal nerves showed degeneration with severe endo- and perineural fibrosis on histology (Masson trichrome stains). No gross or histological lesions were detected after PFA treatments. Ao indicates aorta; LI, left inferior; and RI, right inferior.

Study Limitations

This preclinical animal study is limited due to the differences in anatomy and physiology between canines and humans. For example, PVS peaked in dogs at 2 to 4 weeks and resolved to some extent in individual specimens, but PVS does not resolve in humans. There were only 8 animals included in this study. One animal experienced breathing complications related to anesthesia before undergoing the 8-week CT scan and could not be resuscitated. The PV dimensional data for this animal was truncated at the 4-week time point. The IRF catheter used in this study delivers radiofrequency energy through the tip of the catheter to a ground patch, which is a fundamentally different catheter delivery platform from the array of nine gold electrodes used to deliver PFA. Untreated control vessels used for normalization were significantly smaller than the main branches targeted for ablation, which may be a factor to consider when tracking the treated vessels against the untreated controls. Electrical isolation was not evaluated in this study since the sites chosen for ablations contained limited or no myocardial tissue, preventing any useful electrical assessment of isolation.

Conclusions

Serial CT imaging and 3-dimensional modeling was used to quantitatively evaluate PV stenosis in canines, demonstrating that IRF deliveries resulted in significant PV stenosis, peaking at 2 to 4-weeks after radiofrequency ablation. PFA deliveries had a minimal venous narrowing effect when delivered at proximal sites and deep within the PV anatomy. Vagal nerve, lung tissue, and esophageal injuries were produced by IRF while no such injury was observed from PFA. These findings merit further preclinical studies to evaluate the safety and efficacy of PFA for treatment of AF.

ARTICLE INFORMATION

Received January 8, 2020; accepted June 23, 2020.

Affiliations

Medtronic, Inc, Minneapolis, MN (B.H., N.K., N.B., B.O., S.F., M.T.S.). Oakland University William Beaumont School of Medicine, Royal Oak, MI (D.E.H.). Southlake Regional Health Centre, Newmarket, ON, Canada (A.V.). Mayo Clinic, Rochester, MN (D.P.). University of Ljubljana, Slovenia (D.M.).

Acknowledgments

We thank our colleague Dr Bor Kos for comments that greatly improved the article.

Sources of Funding

This study was fully funded by Medtronic PLC.

Disclosures

Dr Howard, Dr Kirchhof, N. Barka, Dr Onal, S. Fraasch, and M.T. Stewart are employees of Medtronic, Inc. Dr Haines, Dr Verma, and Dr Miklavčič receive research and consultation funds from Medtronic, Inc. The other author report no conflicts.

REFERENCES

- Chugh SS, Havmoeller R, Narayanan K, Singh D, Rienstra M, Benjamin EJ, Gillum RF, Kim YH, McAnulty JH Jr, Zheng ZJ, et al. Worldwide epidemiology of atrial fibrillation: a Global Burden of Disease 2010 Study. *Circulation*. 2014;129:837–847. doi: 10.1161/CIRCULATIONAHA.113.005119
- Miyasaka Y, Barnes ME, Gersh BJ, Cha SS, Bailey KR, Abhayaratna WP, Seward JB, Tsang TS. Secular trends in incidence of atrial fibrillation in Olmsted County, Minnesota, 1980 to 2000, and implications on the projections for future prevalence. *Circulation*. 2006;114:119–125. doi: 10.1161/CIRCULATIONAHA.105.595140
- Krijthe BP, Kunst A, Benjamin EJ, Lip GY, Franco OH, Hofman A, Witteman JC, Stricker BH, Heeringa J. Projections on the number of individuals with atrial fibrillation in the European Union, from 2000 to 2060. *Eur Heart J*. 2013;34:2746–2751. doi: 10.1093/eurheartj/ehd280
- Kok LC, Everett TH 4th, Akar JG, Haines DE. Effect of heating on pulmonary veins: how to avoid pulmonary vein stenosis. *J Cardiovasc Electrophysiol*. 2003;14:250–254. doi: 10.1046/j.1540-8167.2003.02490.x
- Saad EB, Rossillo A, Saad CP, Martin DO, Bhargava M, Erciyes D, Bash D, Williams-Andrews M, Beheiry S, Marrouche NF, et al. Pulmonary vein stenosis after radiofrequency ablation of atrial fibrillation: functional characterization, evolution, and influence of the ablation strategy. *Circulation*. 2003;108:3102–3107. doi: 10.1161/01.CIR.0000104569.96907.7F
- Yu WC, Hsu TL, Tai CT, Tsai CF, Hsieh MH, Lin WS, Lin YK, Tsao HM, Ding YA, Chang MS, et al. Acquired pulmonary vein stenosis after radiofrequency catheter ablation of paroxysmal atrial fibrillation. *J Cardiovasc Electrophysiol*. 2001;12:887–892. doi: 10.1046/j.1540-8167.2001.00887.x
- Robbins IM, Colvin EV, Doyle TP, Kemp WE, Loyd JE, McMahon WS, Kay GN. Pulmonary vein stenosis after catheter ablation of atrial fibrillation. *Circulation*. 1998;98:1769–1775. doi: 10.1161/01.cir.98.17.1769
- Packer DL, Keelan P, Munger B, Breen JF, Asirvatham S, Peterson LA, Monahan KH, Hauser MF, Chandrasekaran K, Sinak LJ, et al. Clinical presentation, investigation, and management of pulmonary vein stenosis complicating ablation for atrial fibrillation. *Circulation*. 2005;111:546–554. doi: 10.1161/01.CIR.0000154541.58478.36
- Calkins H, Hindricks G, Cappato R, Kim YH, Saad EB, Aguinaga L, Akar JG, Badhwar V, Brugada J, Camm J, et al. 2017 HRS/EHRA/ECAS/APHRS/SOLAECE expert consensus statement on catheter and surgical ablation of atrial fibrillation. *Heart Rhythm*. 2017;14:e275–e444. doi: 10.1016/j.hrthm.2017.05.012
- Davalos RV, Mir IL, Rubinsky B. Tissue ablation with irreversible electroporation. *Ann Biomed Eng*. 2005;33:223–231. doi: 10.1007/s10439-005-8981-8
- Rubinsky B, Onik G, Mikus P. Irreversible electroporation: a new ablation modality—clinical implications. *Technol Cancer Res Treat*. 2007;6:37–48. doi: 10.1177/153303460700600106
- Reddy VY, Koruth J, Jais P, Petru J, Timko F, Skalsky I, Hebel R, Labrousse L, Barandon L, Kralovec S, et al. Ablation of atrial fibrillation with pulsed electric fields: an ultra-rapid, tissue-selective modality for cardiac ablation. *JACC Clin Electrophysiol*. 2018;4:987–995.
- Reddy VY, Neuzil P, Koruth JS, Petru J, Funosako M, Cochet H, Sediva L, Chovanec M, Dukkupati SR, Jais P. Pulsed field ablation for pulmonary vein isolation in atrial fibrillation. *J Am Coll Cardiol*. 2019;74:315–326. doi: 10.1016/j.jacc.2019.04.021
- Sugrue A, Vaidya V, Witt C, DeSimone CV, Yasin O, Maor E, Killu AM, Kapa S, McLeod CJ, Miklavčič D, et al. Irreversible electroporation for catheter-based cardiac ablation: a systematic review of the preclinical experience. *J Interv Card Electrophysiol*. 2019;55:251–265. doi: 10.1007/s10840-019-00574-3
- Yarmush ML, Golberg A, Serša G, Kotnik T, Miklavčič D. Electroporation-based technologies for medicine: principles, applications, and challenges. *Annu Rev Biomed Eng*. 2014;16:295–320. doi: 10.1146/annurev-bioeng-071813-104622
- Kotnik T, Rems L, Tarek M, Miklavčič D. Membrane electroporation and electroporation: mechanisms and models. *Annu Rev Biophys*. 2019;48:63–91. doi: 10.1146/annurev-biophys-052118-115451
- van Driel VJ, Neven KG, van Wessel H, du Pré BC, Vink A, Doevendans PA, Wittkamp FH. Pulmonary vein stenosis after catheter ablation: electroporation versus radiofrequency. *Circ Arrhythm Electrophysiol*. 2014;7:734–738. doi: 10.1161/CIRCEP.113.001111
- Witt CM, Sugrue A, Padmanabhan D, Vaidya V, Gruba S, Rohl J, DeSimone CV, Killu AM, Naksuk N, Pederson J, et al. Intrapulmonary vein ablation without stenosis: a novel balloon-based direct current electroporation approach. *J Am Heart Assoc*. 2018;7:e009575.
- Koruth J, Kuroki K, Iwasawa J, Enomoto Y, Viswanathan R, Brose R, Buck ED, Speltz M, Dukkupati SR, Reddy VY. Preclinical evaluation of pulsed

- field ablation: electrophysiological and histological assessment of thoracic vein isolation. *Circ Arrhythm Electrophysiol*. 2019;12:e007781. doi: 10.1161/CIRCEP.119.007781
20. Stewart MT, Haines DE, Verma A, Kirchhof N, Barka N, Grassl E, Howard B. Intracardiac pulsed field ablation: Proof of feasibility in a chronic porcine model. *Heart Rhythm*. 2019;16:754–764. doi: 10.1016/j.hrthm.2018.10.030
 21. Bertacchini C, Margotti PM, Bergamini E, Lodi A, Ronchetti M, Cadossi R. Design of an irreversible electroporation system for clinical use. *Technol Cancer Res Treat*. 2007;6:313–320. doi: 10.1177/153303460700600408
 22. Mali B, Gorjup V, Edhemovic I, Breclj E, Cemazar M, Sersa G, Strazisar B, Miklavcic D, Jarm T. Electrochemotherapy of colorectal liver metastases—an observational study of its effects on the electrocardiogram. *Biomed Eng Online*. 2015;14(suppl 3):S5. doi: 10.1186/1475-925X-14-S3-S5
 23. Kirchhof N. What Is "Preclinical Device Pathology": an introduction of the unfamiliar. *Toxicol Pathol*. 2019;47:205–212. doi: 10.1177/0192623319827502
 24. Raeisi-Giglou P, Wazni OM, Saliba WJ, Barakat A, Tarakji KG, Rickard J, Cantillon D, Baranowski B, Tchou RJ, Bhargava M, et al. Outcomes and management of patients with severe pulmonary vein stenosis from prior atrial fibrillation ablation. *Circ Arrhythm Electrophysiol*. 2018;11:e006001. doi: 10.1161/CIRCEP.117.006001
 25. Padala SK, Ellenbogen KA. Pulmonary vein stenosis after atrial fibrillation ablation: an iatrogenic problem larger than the primary problem. *Circ Arrhythm Electrophysiol*. 2018;11:e006461. doi: 10.1161/CIRCEP.118.006461